they are alkali-rich[31]. This alkali effect is most pronounced at pressures below 20 kbar, however. At 30 kbar, liquids in equilibrium with mantle peridotite are not alkali-rich. The alkali content of experimental slab melts increases with pressure, and comparison with their natural equivalents has shown that slab melting is likely to occur at 30 kbar or more. Thus, besides the physical aspects of magma transport and percolation, any alkali-rich slab melt produced at or beyond 30 kbar, as in our experiments, will be in strong chemical disequilibrium with the overlying mantle wedge. Extensive interaction between these melts and peridotite is expected to occur and the alkali-rich, silica-rich melts will have little opportunity to reach shallower levels unchanged. On this basis, preservation or eruption of genuine slab melts can be anticipated to be difficult, accounting for their relative rarity in most arcs. The chemical differences observed between experimentally produced slab-melts and those erupted or preserved as melt inclusions[32] must in fact reflect various extents of interaction of the latter with mantle material during upward migration. □

Received 22 June 2000; accepted 16 January 2001.

1. Hofmann, A. W. Chemical differentiation of the Earth: the relationships between mantle, continental crust, and oceanic crust. *Earth Planet. Sci. Lett.* **90,** 297–314 (1988).
2. Eiler, J. M., McInnes, B., Valley, J. W., Graham, C. M. & Stolper, E. M. Oxygen isotope evidence for slab-derived fluids in the sub-arc mantle. *Nature* **393,** 777–781 (1998).
3. Nicholls, I. A. & Ringwood, A. E. Effect of water on olivine stability in tholeiites and production of silica saturated magmas in island arc environment. *J. Geol.* **81,** 285–300 (1973).
4. Hawkesworth, C. J., Turner, S. P., McDermott, F., Peate, D. W. & van Calsteren, P. U–Th isotopes in arc magmas: implications for element transfer from the subducted crust. *Science* **276,** 551–555 (1997).
5. Defant, M. J. & Drummond, M. S. Derivation of some modern arc magmas by melting of young subducted lithosphere. *Nature* **347,** 662–665 (1990).
6. Kepezhinskas, P. K., Defant, M. J. & Drummond, M. S. Na metasomatism in the island-arc mantle by slab melt-peridotite interaction: evidence from mantle xenoliths in the north Kamchatka arc. *J. Petrol.* **36,** 1505–1527 (1995).
7. Sorensen, S. S. & Grossman, J. N. Enrichment of trace elements in garnet amphibolites from a paleo-subduction zone: Catalina Schist, southern California. *Geochim. Cosmochim. Acta* **53,** 3155–3177 (1989).
8. Zanetti, A., Mazzucchelli, Rivalenti, G. & Vannucci, R. The Finero phlogopite-peridotite massif: an example of subduction-related metasomatism. *Contrib. Mineral. Petrol.* **134,** 107–122 (1999).
9. Prouteau, G., Scaillet, B., Pichavant, M. & Maury, R. C. Fluid-present melting of ocean crust in subduction zones. *Geology* **27,** 1111–1114 (1999).
10. Peacock, S. M., Rushmer, T. & Thompson, A. B. Partial melting of subducting oceanic crust. *Earth Planet. Sci. Lett.* **121,** 227–244 (1994).
11. Whinter, K. T. & Newton, R. C. Experimental melting of hydrous low-K tholeiite: evidence on the origin of Archean cratons. *Bull. Geol. Soc. Denmark* **39,** 213–228 (1991).
12. Spulber, S. D. & Rutherford, M. J. The origin of rhyolite and plagiogranite in oceanic crust: an experimental study. *J. Petrol.* **24,** 1–25 (1983).
13. Beard, J. S. & Lofgren, G. E. Dehydration melting and water-saturated melting of basaltic and andesitic greenstones and amphibolites at 1, 3, and 6.9 kb. *J. Petrol.* **32,** 365–401 (1991).
14. Rapp, R. P. & Watson, E. B. Dehydration melting of metabasalt at 8–32 kbar: implications for continental growth and crust-mantle recycling. *J. Petrol.* **36,** 891–931 (1995).
15. Sen, C. & Dunn, T. Dehydration melting of a basaltic composition amphibolite at 1.5 and 2.0 GPa: implications for the origin of adakites. *Contrib. Mineral. Petrol.* **117,** 394–409 (1994).
16. Ryerson, F. J. & Watson, E. B. Rutile saturation in magmas: implications for Ti-Nb-Ta depletion in island-arc basalts. *Earth Planet. Sci. Lett.* **86,** 225–239 (1987).
17. Ulmer, P. & Trommsdorff, V. Serpentinite stability to mantle depths and subduction-related magmatism. *Science* **268,** 858–861 (1995).
18. Schmidt, M. & Poli, S. Experimentally based water budget for dehydrating slabs and consequences for arc magma generation. *Earth Planet. Sci. Lett.* **163,** 361–379 (1998).
19. Atherton, M. P. & Petford, N. Generation of sodium-rich magmas from newly underplated basaltic crust. *Nature* **362,** 144–146 (1993).
20. Carroll, M. J. & Wyllie, P. J. Experimental phase relations in the system peridotite-tonalite-H_2O at 15 kbar: implications for assimilation and differentiation processes at the crust-mantle boundary. *J. Petrol.* **30,** 1351–1382 (1989).
21. Sen, C. & Dunn, T. Experimental modal metasomatism of a spinel lherzolite and the production of amphibole-bearing peridotite. *Contrib. Petrol. Mineral.* **119,** 422–432 (1994).
22. Rapp, R. P., Shimizu, N., Norman, M. D. & Applegate, G. S. Reaction between slab-derived melts and peridotite in the mantle wedge: experimental constraints at 3.8 GPa. *Chem. Geol.* **160,** 335–356 (1999).
23. Kelemen, P., Shimizu, N. & Dunn, T. Relative depletion of niobium in some arc magmas and the continental crust: partitioning of K, Nb, La, and Ce during melt/rock reaction in the upper mantle. *Earth Planet. Sci. Lett.* **120,** 111–134 (1993).
24. Yogodinzski, G. M., Volynets, O. N., Koloskov, A. V. & Seliverstov, N. I. Magnesian andesites and the subduction component in a strongly calcalkaline series at Piip volcano, far western Aleutian. *J. Petrol.* **34,** 163–204 (1994).
25. Ionov, D. A. & Hofmann, A. W. Nb-Ta-rich mantle amphiboles and micas: implications for subduction-related metasomatic trace element fractionations. *Chem. Geol.* **131,** 341–356 (1995).
26. Martin, H. Effect of steeper Archean geothermal gradient on geochemistry of subduction zone magmas. *Geology* **14,** 753–756 (1986).
27. Drummond, M. S., Defant, M. J. & Kepezhinskas, P. K. Petrogenesis of slab derived-tonalite-dacite adakite magmas. *Trans. R. Soc. Edinburgh* **87,** 205–215 (1996).
28. Schneider, M. E. & Eggler, D. H. Fluids in equilibrium with peridotite minerals: implications for mantle metasomatism. *Geochim. Cosmochim. Acta* **50,** 711–724 (1986).
29. Tatsumi, Y. Migration of fluid phases and genesis of basalt magmas in subduction zones. *J. Geophys. Res.* **94,** 4697–4707 (1989).
30. Eiler, J. M. *et al.* Oxygen isotopes geochemistry of oceanic-arc lavas. *J. Petrol.* **41,** 229–256 (2000).
31. Hirschman, M. M., Baker, M. B. & Stolper, E. M. The effect of alkalis on the silica content of mantle-derived melts. *Geochim. Cosmochim. Acta* **62,** 883–902 (1998).
32. Schiano, P. *et al.* Hydrous, silica-rich melts in the sub-arc mantle and their relationship with erupted arc-lavas. *Nature* **377,** 595–600 (1995).

Correspondence and requests for materials should be addressed to B.S. (e-mail: bscaille@cnrs-orleans.fr).

Branched integumental structures in *Sinornithosaurus* and the origin of feathers

Xing Xu*, Zhong-he Zhou* & Richard O. Prum†

** Institute of Vertebrate Paleontology and Paleoanthropology, Academica Sinica, PO Box 643, Beijing, 100044, People's Republic of China*
† Department of Ecology and Evolutionary Biology, and Natural History Museum, University of Kansas, Lawrence, Kansas 66045, USA

The evolutionary origin of feathers has long been obscured because no morphological antecedents were known to the earliest, structurally modern feathers of *Archaeopteryx*[1]. It has been proposed that the filamentous integumental appendages on several theropod dinosaurs are primitive feathers[2–6]; but the homology between these filamentous structures and feathers has been disputed[7–9], and two taxa with true feathers (*Caudipteryx* and *Protarchaeopteryx*) have been proposed to be flightless birds[8,10]. Confirmation of the theropod origin of feathers requires documentation of unambiguously feather-like structures in a clearly non-avian theropod. Here we describe our observations of the filamentous integumental appendages of the basal dromaeosaurid dinosaur *Sinornithosaurus millenii*, which indicate that they are compound structures composed of multiple filaments. Furthermore, these appendages exhibit two types of branching structure that are unique to avian feathers: filaments joined in a basal tuft, and filaments joined at their bases in series along a central filament. Combined with the independent phylogenetic evidence supporting the theropod ancestry of birds[11–13], these observations strongly corroborate the hypothesis that the integumental appendages of *Sinornithosaurus* are homologous with avian feathers. The plesiomorphic feathers of *Sinornithosaurus* also conform to the predictions of an independent, developmental model of the evolutionary origin of feathers[14].

Sinornithosaurus millenii (Fig. 1) is a non-avian, basal dromaeosaurid dinosaur from the Lower Cretaceous Yixian formation (~124.6 Myr ago), Liaoning, China[5]. Along with *Sinosauropteryx*[3] (a basal coelurosaur), *Beipiaosaurus*[4] (a therizinosauroid) and *Microraptor*[6] (a dromeosaur), *Sinornithosaurus*[5] has many filamentous integumental structures that may be plesiomorphic feathers. As in *Beipiaosaurus* and *Microraptor*, the filamentous integumental appendages of *Sinornithosaurus* are indistinguishable from the contour feathers of birds preserved in the same deposits (compared with holotypes of *Confuciusornis sanctus, Eoenantiornis buhler* and *Chanchengornis hengdaoziensis*). In these avian specimens, the indisputable contour feathers on the body are preserved as diffuse arrays of filaments of varying diameters without a prominent rachis or central shaft. Despite these similarities, homology between the

integumental filaments of *Sinornithosaurus* and avian feathers has been questioned[9].

Further preparation of the holotype of *Sinornithosaurus* (IVPP V12811) has revealed new details about the morphology of its filamentous integumental appendages, which are preserved as carbonized filaments around the specimen (Fig. 1). The appendages are generally 30–45 mm long and 1–3 mm wide. Many appendages remain closely associated with the integument of the skull, neck, forelimbs, legs and tail. Others were dissociated from the integument and are preserved in the matrix around the specimen. No remiges or rectrices (that is, flight feathers) with prominent rachi have been observed. These appendages are unlikely to be collagenous dermal or musculoskeletal structures[7] because they are clearly preserved as external integumental structures. Furthermore, they are too numerous and broadly distributed to be partially ossified tendons.

Avian feathers are characterized by a complex, branched structure of keratinaceous filaments that grow by a unique mechanism from cylindrical feather follicles[14,15]. This branching structure is the most distinctive morphological feature of feathers. Our observations indicate that there are similar branching structures in the integumental appendages of *Sinornithosaurus*. Generally, the *Sinornithosaurus* appendages are preserved not as solitary fibres but as compound structures containing multiple filaments (Fig. 2). This compound filamentous structure is particularly notable in appendages that were dissociated from the body during preservation and deposited around the specimen (Fig. 2). The preservation of numerous, randomly oriented, compound structures overlying each other shows that these integumental appendages were dissociated from the skin and from one another before preservation, but that the component filaments within each appendage remained associated (Fig. 2), indicating that the component filaments in each appendage were joined together. In contrast, single, unbranched, independent, hair-like integumental filaments would be unlikely to be preserved in similarly sized groups of overlying filaments. Multiple hair-like filaments from independent integumental structures might remain associated if they were attached to a single piece of skin that sloughed off the body during decomposition, but the varying orientation of the dissociated, overlying *Sinornithosaurus* appendages (Fig. 2) argues directly against this interpretation.

In addition to their compound structure, the integumental appendages of *Sinornithosaurus* exhibit two types of feather-like

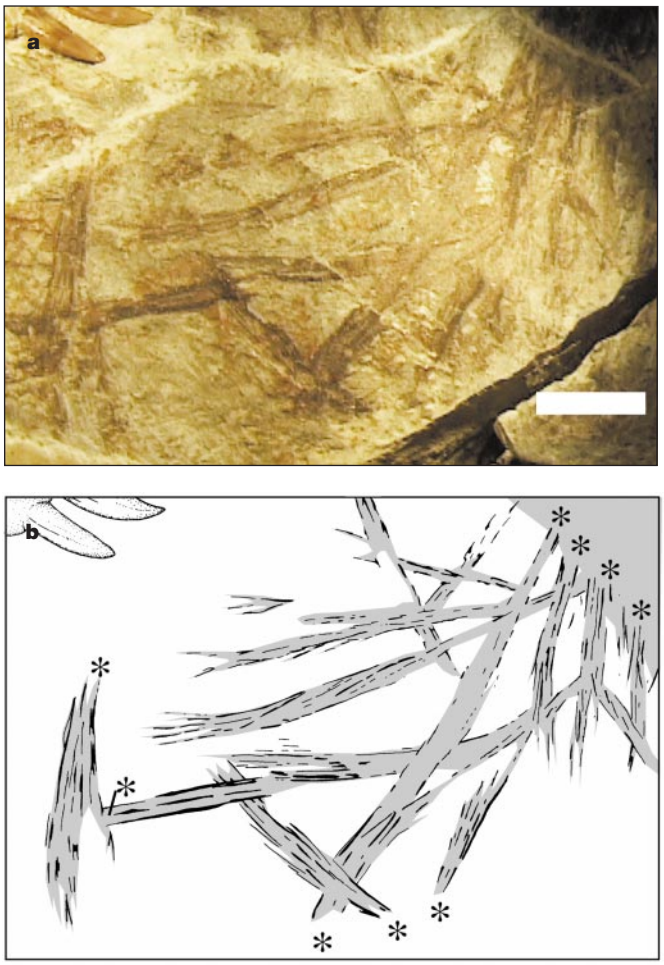

Figure 2 Filamentous integumental appendages of *S. millenii* dissociated from the integument and preserved overlying each other in the matrix near the skull. **a**, Picture of the preparation. Scale bar, 5 mm. **b**, Illustrated reconstruction of the appendages showing the positions of the observed filaments (lines) and the inferred outline of the appendages (shading). Asterisks, the proximal ends of each appendage. Each appendage is composed of multiple component filaments.

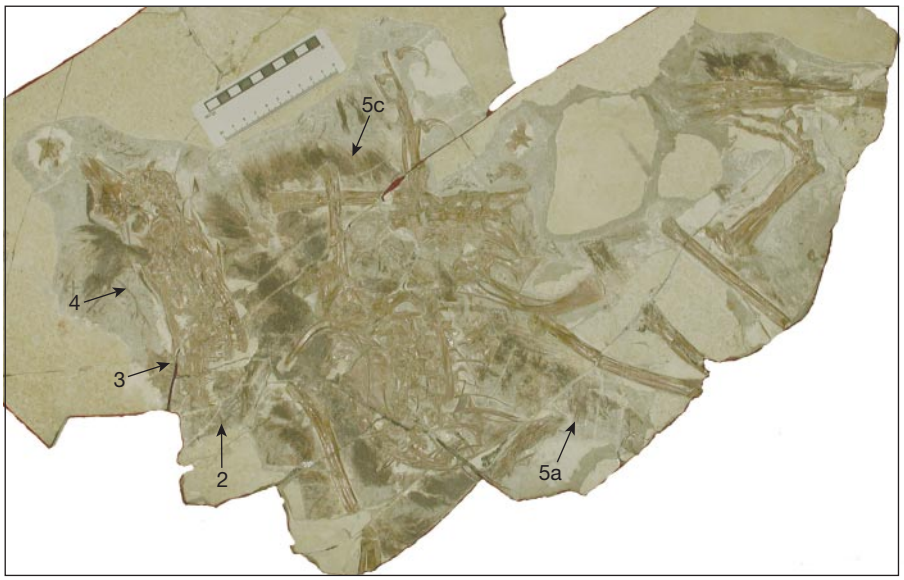

Figure 1 *Sinornithosaurus millenii*, holotype (IVPP 12811). Carbonized, filamentous, integumental appendages, 30–45 mm long, are attached to the skull, forelimbs, tail and other skeletal elements. Dissociated appendages are preserved in the substrate around the specimen. The locations of the appendages illustrated in subsequent Figures are labelled with the corresponding Figure numbers.

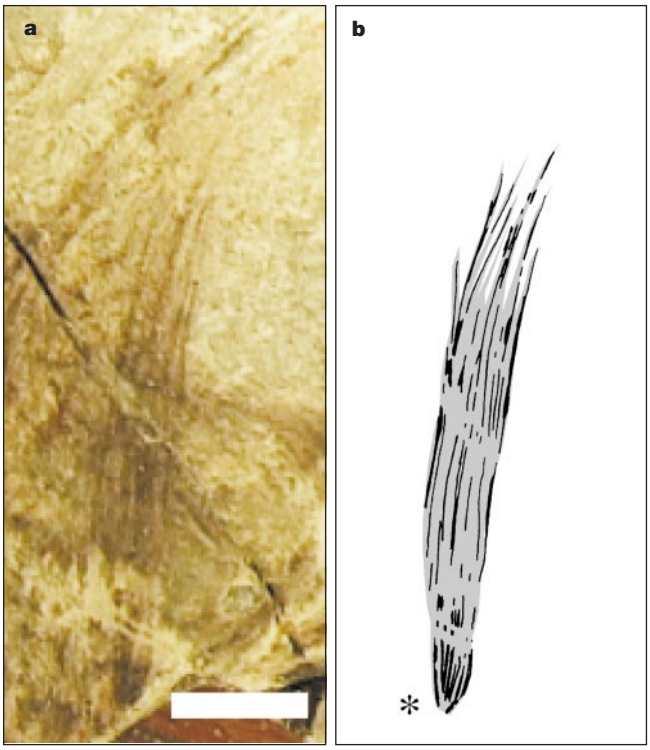

Figure 3 Filamentous integumental appendage of *S. millenii* from the dorsal surface of the snout. **a**, Picture of the preparation. Scale bar, 5 mm. **b**, Illustrated reconstruction of the appendage showing the positions of the observed filaments (lines) and the inferred outline of the appendage (shading). Asterisk, the proximal end of the appendage. The nearly parallel fibres converge at the base on a single point.

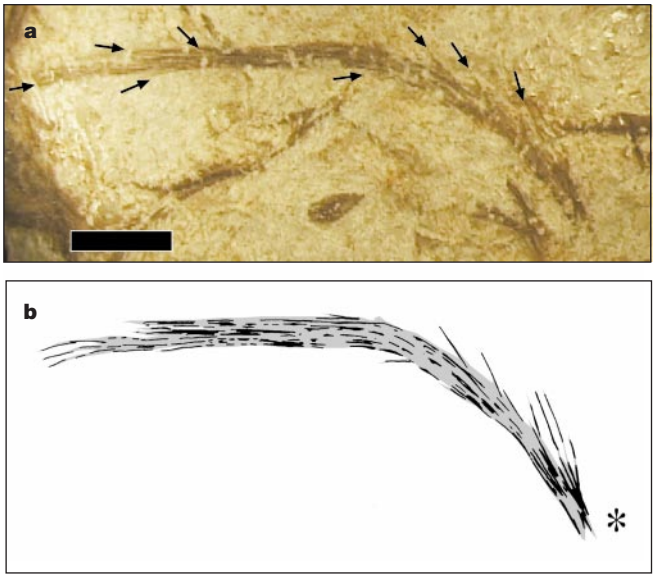

Figure 4 Dissociated filamentous integumental appendage of *S. millenii* from near the skull. **a**, Arrows indicate the distal tips of some component filaments. Scale bar, 5 mm. **b**, Illustrated reconstruction of the appendage showing the positions of the observed filaments (lines) and the inferred outline of the appendage (shading). Asterisk, the proximal end of the appendage. The curved position of the appendage reveals its compound structure. Each filament converges on the centre of the appendage at its base.

branching structure. In several instances, component filaments are generally similar in length, extensively parallel for most of their length, and converge conspicuously at their bases on a single point (Fig. 3). In this form of branched structure, many unbranched filaments converge on a single point in a prominent tuft.

One dissociated integumental appendage is preserved in a curved position that demonstrates a second form of branched structure (Fig. 4). Here, the distal tips of the component filaments occur along the entire length of the appendage, and the filaments form the margins of the appendage in a manner similar to a pennaceous feather vane. Furthermore, the component filaments are not parallel to the central axis of the appendage as it curves. Rather, filaments from both sides are straighter than the appendage as whole, and each filament converges at its base on the central midline of the composite appendage. This conformation would be expected only for filaments that were joined at their bases to other filaments or to a central filament (or shaft). These observations are not consistent with a frayed, fibrous composite material (for example, ossified tendon) because the appendage remains essentially the same width throughout its length even though new filaments are consistently added to it. The distal filaments could not continue all the way to the base of the appendage at their observed diameters or the width of the appendage would increase substantially as new filaments were added. As the component filaments are not as long as the appendage itself, it appears that they are joined at their bases to another filament within the appendage.

In several instances, there are additional indications of a larger central filament and secondary branches within a single appendage. Some appendages display a general outline of the margins of the appendage with a substantially larger, darker, more prominent filament running down the centre (Fig. 5a, b). In one instance, a single filament can be seen joining at its base to the larger central filament at an acute angle (Fig. 5a, b), in the manner of the rachis and barbs of a pinnate feather. The filamentous integumental appendages along the right ulna are preserved as a substantial mat of filaments (Fig. 5c). The heterogeneous filaments differ strikingly in diameter and in angle to the ulna, consistent with impressions of many fibres from different but closely associated branched appendages. The longest, darkest and thickest filaments are straight, perpendicular to the skin, and arrayed along the ulna at regular distances (around 0.5 mm apart). These larger filaments are also largest at their bases.

The integumental appendages of *Sinornithosaurus* are compound structures composed of multiple filaments with two types of branched structure. First, the tufts of filaments joined at their bases are identical in structure to avian natal down feathers in which multiple filamentous barbs are basally fused to a single calamus[15]. Among modern vertebrate integumental appendages, this type of branched structure is unique to avian feathers[15]. (Chinchilla (Chinchillidae) hair is also tufted, but each filament actually grows from an independent root within a follicle[16,17].) Second, the serial branching of filaments along a central shaft is identical in structure to the barbs and the rachis of a pennaceous feather, and is also unique to avian feathers. The integumental appendages of *Sinornithosaurus* are different from most modern avian feathers in their apparent lack of barbules. Thus, *Sinornithosaurus* appendages could not have formed a closed pennaceous vane.

The compound filamentous structure and the two types of feather-like branching in the integumental appendages of *Sinornithosaurus* strongly indicate that these structures are homologous with avian feathers. A previous phylogenetic analysis[5] indicates that *Sinornithosaurus* is not a bird but is a basal lineage of the dromaeosaurids which, by themselves or in combination with troodontids, have been repeatedly considered to be the lineage of theropods most closely related to birds[11–13]. Thus, the proposed homology between the integumentary appendages of *Sinornithosaurus* and avian feathers is supported by observations of detailed, derived morphological similarities, and is strongly

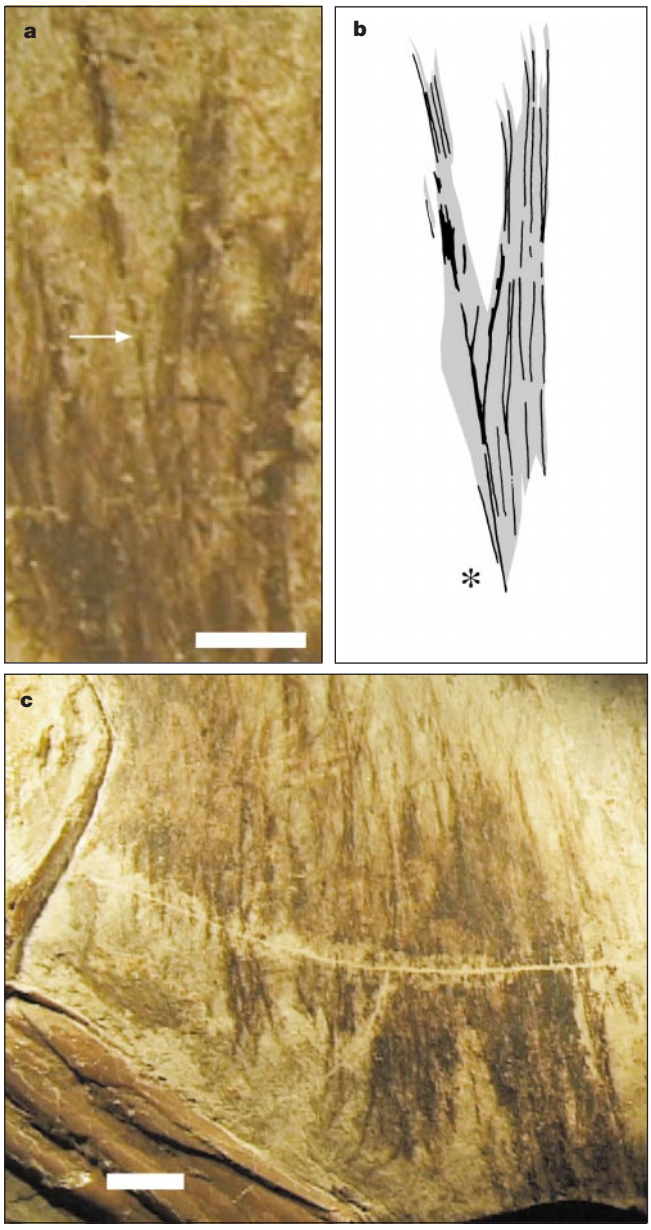

Figure 5 Filamentous integumental appendages of *S. millenii* indicating the presence of larger central filaments, or shafts, and secondary branched filaments. **a**, Dissociated appendages from near the left femur. Arrow indicates where a secondary filament joins at its base at an acute angle to a larger central filament. **b**, Illustrated reconstruction of the appendage showing the positions of the observed filaments (lines) and the inferred outline of the entire appendages (shading). Asterisk, the proximal end of the appendages. **c**, Filamentous integumental appendages preserved in nearly their original positions along the right ulna. Scale bars, 5 mm.

corroborated by independent phylogenetic data showing that these lineages are historically closely related.

The morphology of the plesiomorphic feathers of *Sinornithosaurus* is also congruent with the predictions of an independent, developmental model of the evolutionary origin of feathers[14]. This developmental model proposes that feathers originated with the evolution of the first cylindrical feather follicle, and that they subsequently evolved through a series of derived novelties in the developmental mechanisms within the follicle[14]. The model predicts a transition series of feather morphologies from the first hollow, cylindrical feather through all modern feather structural diversity[14] (Fig 6). The two appendage morphologies observed

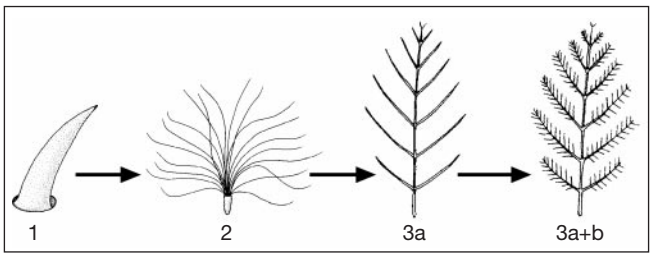

Figure 6 The predicted transition series of feather morphologies from an independent, developmental model of the evolutionary origin of feathers[14]. The model[14] hypothesizes that the first feather originated with the first follicle—a cylindrical epidermal invagination around a papilla. Subsequent feather diversity evolved through a series of derived novelties in the developmental mechanisms within the follicle. The integumental appendages of *Sinornithosaurus* described here are congruent with Stages II and IIIa, whereas the integumental appendages of *Sinosauropteryx*[2] are congruent in morphology with Stage I. Stage I, an unbranched, hollow filament; Stage II, a tuft of barbs basally fused to a calamus; Stage IIIa, a feather with a rachis and serially fused barbs; Stage IIIa+b, a feather with rachis, barbs and barbules. Stage IV (not shown), a bipinnate feather with differentiated distal and proximal barbules and a closed pennaceous vane; Stage Va–f (not shown), additional modern feather diversity including asymmetrical flight feathers.

in *Sinornithosaurus* are exactly congruent with the Stage II and Stage IIIa morphologies predicted by this model (Fig. 6). Furthermore, the shorter, unbranched integumental appendages of *Sinosauropteryx*[2], a basal coelurosaur, are also congruent with the predicted Stage I feather morphology (Fig. 6). The morphologies and phylogenetic distributions of these theropod integumental appendages conform closely to the ancestral feather morphologies predicted by the developmental model of the origin of feathers[14].

These results support the hypothesis that feathers evolved and initially diversified in terrestrial theropod dinosaurs before the origin of birds and flight. Furthermore, feathers evolved filamentous structure, basal branching, and a rachis with barbs before they evolved bipinnate structure, differentiated proximal and distal barbules, and the closed pennaceous vane that are required for aerodynamic function. Contrary to recent reports[18], the hypothesis of the theropod origin of feathers is strongly corroborated by fossil observations and phylogenetic analyses. □

Received 2 August; accepted 19 December 2000.

1. de Beer, G. Archaeopteryx lithographica; *A Study Based on the British Museum Specimen* (Trustees of the British Museum, London, 1954).
2. Chen, P.-J., Dong, Z. M. & Zhen, S. N. An exceptionally well-preserved theropod dinosaur from the Yixian formation of China. *Nature* **391,** 147–152 (1998).
3. Ji, Q., Currie, P. J., Norell, M. A. & Ji, S.-A. Two feathered dinosaurs from northeastern China. *Nature* **393,** 753–761 (1998).
4. Xu, X., Tang, Z.-l. & Wang, X.-l. A therizinosauroid dinosaur with integumentary structures from China. *Nature* **399,** 350–354 (1999).
5. Xu, X., Wang, X.-l. & Wu, X.-C. A dromaeosaurid dinosaur with a filamentous integument from the Yixian Formation of China. *Nature* **401,** 262–266 (1999).
6. Xu, X., Zhou, Z. & Wang, X. The smallest known non-avian theropod dinosaur. *Nature* **408,** 705–708 (2000).
7. Gibbons, A. Plucking the feathered dinosaur. *Science* **278,** 1229–1230 (1997).
8. Feduccia, A. *The Origin and Evolution of Birds* 2nd edn (Yale Univ. Press, New Haven, 1999).
9. Dalton, R. Feathers fly in Beijing. *Nature* **405,** 992 (2000).
10. Jones, T. D., Farlow, J. O., Ruben, J. A., Henderson, D. M. & Hillenius, W. J. Cursoriality in bipedal archosaurs. *Nature* **406,** 716–718 (2000).
11. Gauthier, J. A. Saurischian monophyly and the origin of birds. *Mem. California Acad. Sci.* **8,** 1–55 (1986).
12. Holtz, T. R. The phylogenetic position of the Tyrannosauridae: implications for theropod systematics. *J. Paleontol.* **68,** 1100–1117 (1994).
13. Sereno, P. The evolution of dinosaurs. *Science* **284,** 2137–2147 (1999).
14. Prum, R. O. Development and evolutionary origin of feathers. *J. Exp. Zool. Mol. Dev. Evol.* **285,** 291–306 (1999).
15. Lucas, A. M. & Stettenheim, P. R. *Avian Anatomy—Integument* (US Dept. Agriculture Handbook, Washington DC, 1972).
16. Nowak, R. M. & Paradiso, J. L. *Walker's Mammals of the World* (Johns Hopkins Univ. Press, Baltimore, 1983).
17. Grau, V. J. *Biología y Patología de la Chinchilla* (Ediciones OIKOS, Santiago, Chile, 1994).
18. Jones, T. A. *et al.* Non-avian feathers in a late Triassic archosaur. *Science* **288,** 2202–2205 (2000).

Acknowledgements

We thank M. Chang and Y. Wang for assistance during the work; S.-h. Xie for preparation of the holotype specimen of *Sinornithosaurus*; and members of the Liaoxi expedition team of the IVPP, who participated in the excavation of the specimen. The paper benefited from discussions with C.-M. Chuong, P. Currie, A. Deane, L. Martin, B. Timm, G. Wagner, L. Witmer and F. Zhang; and was improved by comments from W. Boles, P. Stettenheim and L. Witmer. We acknowledge financial support from the Chinese Academy of Sciences, Chinese Natural Science Foundation, Chinese Special Funds for Major State Basic Research Projects (X.X., Z.Z.), and the United States National Science Foundation (R.O.P.). Order of authorship was assigned randomly.

Correspondence and requests for materials should be addressed to R.O.P. (e-mail: prum@ukans.edu).

Sexual swellings advertise female quality in wild baboons

Leah G. Domb*† & Mark Pagel‡

** Department of Anthropology, Harvard University, Cambridge, Massachusetts 02138, USA*
‡ School of Animal and Microbial Sciences, University of Reading, Whiteknights, Reading RG6 6AJ, UK

The females of many Old World primate species produce prominent and conspicuous swellings of the perineal skin around the time of ovulation. These sexual swellings have been proposed to increase competition among males for females[1] or to increase the likelihood of a female getting fertilized, by signalling either a female's general reproductive status[1–5], or the timing of her ovulation[6]. Here we show that sexual swellings in wild baboons reliably advertise a female's reproductive value over her lifetime, in accordance with a theoretical model of honest signalling[7]. Females with larger swellings attained sexual maturity earlier, produced both more offspring and more surviving offspring per year than females with smaller swellings, and had a higher overall proportion of their offspring survive. Male baboons use the size of the sexual swelling to determine their mating effort, fighting more aggressively to consort females with larger swellings, and spending more time grooming these females. Our results document an unusual case of a sexually selected ornament in females, and show how males, by mating selectively on the basis of the size of the sexual swelling, increase their probability of mating with females more likely to produce surviving offspring.

The females of most Old World primate species with sexual swellings live in multi-male breeding systems, in which females typically mate with more than one male during oestrus[1,2,4]. Theoretical models show that male–male competition for females is inevitable in these circumstances[7], raising the issue of why females produce such exaggerated displays.

One of us (L.G.D.) investigated the function of sexual swellings in a population of wild olive baboons (*Papio cynocephalus anubis*) living in Gombe National Park, Tanzania. This population has been studied extensively since 1967 (refs 8–16). Olive baboons reside in troops of adult males and females, and their juvenile and infant offspring. Most males are immigrants as females remain in their natal territories, and the breeding system is multi-male such that each female typically mates with more than one male per oestrous cycle.

Twenty-nine parous females for which long-term demographic data were available were followed in the wild for 13 months. Measurements of the size of females' sexual swellings and of the behaviour of males towards females were collected for 22 females in 44 oestrus cycles. All male behaviour and sexual swelling-size data are from the 5 days before swelling detumescence in females. For the same females, we extracted from long-term demographic records information on four variables related to fitness: age at first conception; the number of offspring produced per year; the number of surviving offspring produced per year; and the proportion of a female's offspring that survived (see Methods).

Figure 1 shows an example of a baboon sexual swelling in its fully swollen state. We characterized each female's swelling by measuring its length, width and depth. Neither width nor depth of swellings was consistently related to the four indicators of female reproductive value (Table 1), and so hereafter we report only associations with length ('swelling size').

Length of a female's swelling correlates with measures of female fitness (Table 1): females with larger swellings begin to reproduce at an earlier age ($P < 0.005$), produce a larger number of offspring per year ($P < 0.01$) and a larger number of surviving offspring per year ($P < 0.025$); in addition, a greater proportion of their offspring survive ($P < 0.065$). All P values we report are for two-tailed tests. A female's swelling size was related to her age ($r = -0.61$, $P < 0.01$; $n = 22$), but not to her social rank ($r = 0.087$, $n = 18$). We nevertheless controlled statistically for both variables (Table 1). These analyses show that the relationships between the measures of female reproductive value and swelling size remain significant, and in some cases are strengthened. When controlling for female age and rank, swelling size is strongly correlated with the proportion of a female's offspring that survive ($P < 0.025$, Table 1). Size of the oestrous swelling therefore seems to be an indicator of a female's lifetime reproductive value, independently of age and social rank within the troop.

An important component of lifetime reproductive value is the probability of conceiving in each cycle. In humans, early maturing girls have higher frequencies of ovulation than later maturing girls, and higher levels of ovarian steroids in each cycle[17]. Early maturation also has been found in humans to be associated with better reproductive performance throughout a female's life[18–19]. Among females in our study, age of first conception, in addition to being associated with larger swelling size, is significantly associated with a higher number of both offspring produced per year ($r = -0.43$, $P < 0.05$; $n = 29$) and surviving offspring produced per year, relative to other troop members ($r = -0.55$, $P < 0.01$; $n = 29$). Larger swellings signal not only that the female started reproducing earlier, but also that she has a higher reproductive rate relative to other group members. In a mating system such as that of olive baboons in

Figure 1 A baboon sexual swelling showing the fully swollen state.

† Present address: 38 Sydenham Road, Bristol BS6 5SJ, U.K.